Modified power law cosmology: theoretical scenarios and observational constraints

Lokesh Kumar Sharma,[1,*] Suresh Parekh,[2,†] Kalyani C.K. Mehta,[3,‡] Saibal Ray,[4,§] and Anil Kumar Yadav[5,¶]

[1]*Department of Physics, GLA University, Mathura 281406, Uttar Pradesh, India*
[2]*Department of Physics, SP Pune University, Pune 411007, Maharastra, India*
[3]*Department of Physics, Eberhard Karls University of Tubingen, Germany*
[4]*Centre for Cosmology, Astrophysics and Space Science (CCASS), GLA University, Mathura 281406, Uttar Pradesh, India*
[5]*Department of Physics, United College of Engineering and Research, Greater Noida 201 306, India*

This research paper examines a cosmological model in flat space-time via $f(R,G)$ gravity where R and G are respectively the Ricci scalar and Gauss-Bonnet invariant. Our model assumes that $f(R,G)$ is an exponential function of G combined with a linear combination of R. We scrutinize the observational limitations under a power law cosmology that relies on two parameters - H_0, the Hubble constant, and q, the deceleration parameter, utilizing the 57-point $H(z)$ data, 8-point BAO data, 1048-point Pantheon data, joint data of $H(z)$ + Pantheon, and joint data of $H(z)$ + BAO + Pantheon. The outcomes for H_0 and q are realistic within oberservational ranges. We have also addressed Energy Conditions, $Om(z)$ analysis and cosmographical parameters like Jerk, Lerk and Snap. Our estimate of H_0 is remarkably consistent with various recent Planck Collaboration studies that utilize the ΛCDM model. According to our study, the power law cosmology within the context of $f(R,G)$ gravity provides the most comprehensive explanation for the important aspects of cosmic evolution.

I. INTRODUCTION

Strong evidence for the universe's accelerated expansion is provided by several current standard observations, e.g. type Ia Supernovae (SNeIa), the cosmic microwave background (CMB) radiation, large scale structure (LSS), the Planck satellite, baryon acoustic oscillations (BAO) and the Wilkinson microwave anisotropy probe (WMAP). It is observed that modified gravity could provide a more accurate description of the universe's accelerating expansion. As far as we are aware, modified gravity offers a straightforward gravitational substitute for the dark energy paradigm. These theories of dark energy are based on expanding the Einstein-Hilbert action with gravitational components. This has the effect of altering the universe's evolution, either early or late. In modified gravity, there are numerous examples of these models in the literature [1–3]. The universe expanded at an incredibly fast rate during the inflationary phase. The discovery of the inflationary era in the late 1970s and early 1980s helped to resolve some of the Big Bang model's issues. Cosmological models that bounce could be a valid explanation for the universe at both early and late times, according to evidence. A uniform description of this could be provided by modified gravity. A phantom fluid or field is needed to explain the accelerated expansion in standard general relativity. Ultimately, this phantom field results in a large rupture or a singularity of the crushing kind [4].

Modified gravity is another explanation for the universe's late-time acceleration. In the initial phase $f(R)$ gravity has been exploited with R in the Einstein-Hilbert action which is the scalar curvature. This notion is easy to understand, workable and very effective. However, at present General Relativity (GR) has numerous variations. As a result we obtain $f(R,T)$ theory if the Lagrangian is a function of both R and the energy-momentum tensor's trace T [5–27]. In this gravity theory, some of the basic aspects are as follows: (i) here the trace of the energy-momentum tensor T and (ii) the Ricci scalar R which have considerable intrinsic features to the matter Lagrangian. Moreover, the quantum field effect as well as the particle creation potentiality are some other attributes to $f(R,T)$ gravity. All these aspects of modified gravity theories are available in the following review work [28]. In order to account for heat conduction, viscosity, and quantum effects, the T term is introduced. There is another explanation for the late time cosmic acceleration. Observational restrictions have been applied to $f(R,T)$ gravity. However, $f(R,G)$ gravity

* lokesh.sharma@gla.ac.in
† thesureshparekh@gmail.com
‡ kalyani.c.k.mehta@gmail.com
§ saibal.ray@gla.ac.in
¶ abanilyadav@yahoo.co.in

presents an intriguing substitute for $f(R)$ gravity and G referes to the Gauss-Bonnet invariant. Numerous studies in the literature demonstrate that inflation and late-time acceleration can be explained by $f(R,G)$ gravity [29–42]. Here, the analysis of the universe's physical properties in $f(R,G)$ gravity is our primary goal.

Understanding of the late-time acceleration of the universe is largely dependent on the mainstream cosmological model. However, a wide variety of models explaining the primary characteristics of the cosmos may be found in the literature. Age, horizon, and fuzziness issues in the standard model are successfully resolved by models based on a power-law of the scale factor [43–46]. In general the expansion rate of the universe is described by the Hubble constant H_0. In the recent past, we have observed the statistically significant tensions in H_0 which refers to the difference between its direct local distance ladder measurements and consideration of the standard ΛCDM model. For example there is approximately 4.4 σ tension in value of H_0 determined by SH0ES measurement $H_0 = 73.04 \pm 1.04\,\mathrm{km\,s^{-1}\,Mpc^{-1}}$ (68% CL) [47] and $H_0 = 67.27 \pm 0.60\,\mathrm{km\,s^{-1}\,Mpc^{-1}}$ (68% CL) [48]. This discrepancy in the value of H_0 is referred as H_0 tension. Some important researches on H_0 tension are given in Refs. [49–61].

In view of the above mentioned motivation, the plan of the present study is outlined as: in Section II, a brief mathematical overview of the metric and $f(R,G)$ gravity theory along with the solution to the field equations have been provided. In Section III, observational analysis has been executed within the observational constraints of the model parameters. The physical parameters involved in the model are presented by the help of plots in Section IV. At last, Section V is designed for relevant comments on the entire investigation.

II. THE ACTION AND COSMOLOGICAL SOLUTIONS

A. Field Equations

In four-dimensional space-time, the modified Gauss-Bonnet gravity operates as

$$S = \int \left[\frac{f(R,G)}{2\kappa}\right] \sqrt{-g} d^4x + S_m, \tag{1}$$

where $\kappa = 8\pi G$ and S_m is the matter Lagrangian which depends upon $g_{\mu\nu}$ and matter fields. The Gauss-Bonnet invariant G is defined as $G = R^2 + R_{\mu\nu\alpha\zeta}R^{\mu\nu\alpha\zeta} - 4R_{\mu\nu}R^{\mu\nu}$. The Gauss-Bonnet invariant is obtained from $R_{\mu\nu\alpha\zeta}$, $R_{\mu\nu} = R^{\zeta}_{\mu\zeta\nu}$ and $R = g^{\alpha\zeta}R_{\alpha\zeta}$.

From Eq. (1), the gravitational field equations are derived as

$$\begin{aligned} &R_{\mu\nu} - \frac{1}{2}F(G) + (2RR_{\mu\nu} - 4R_{\mu\alpha}R^{\alpha}_{\nu} + 2R^{\alpha\zeta\tau}_{\mu}R_{\nu\alpha\zeta\tau} - 4g^{i\alpha}G^{i\zeta}R_{\mu i\nu j}R_{\alpha\zeta})F'(G) \\ &+ 4[\nabla_{\alpha}\nabla_{\nu}F'(G)]R^{\alpha}_{\mu} - 4g_{\mu\nu}[\nabla_{\alpha}\nabla_{\zeta}F'(G)]R^{\alpha\zeta} + 4[\nabla_{\alpha}\nabla_{\zeta}F'(G)]g^{i\alpha}g^{j\zeta}R^{\mu}_{ivj} \\ &+ 2g_{\mu\nu}[\Box F'(G)]R - 2[\nabla_{\mu}\nabla_{\nu}F'(G)]R - 4[\Box F'(G)]R_{\mu\nu} + 4[\nabla_{\mu}\nabla_{\alpha}F'(G)]R^{\alpha}_{\nu} = \kappa T^{m}_{\mu\nu}, \end{aligned} \tag{2}$$

where T^{m}_{ij} is the energy momentum tensor arising from S_m.

The flat FLRW space-time metric is

$$ds^2 = -dt^2 + a^2(t)(dx^2 + dy^2 + dz^2), \tag{3}$$

where the symbols have their usual meanings. Now, we calculate the Einstien field equations using 2 and 1 as

$$F(G) + 6H^2 - GF'(G) + 24H^3\dot{G}F''(G) = 2\kappa\rho, \tag{4}$$

$$6H^2 + 4\dot{H} + F(G) + 16H\dot{G}(\dot{H} + H^2)F''(G) - GF'(G) + 8H^2\ddot{G}F''(G) + 8H^2\dot{G}^2F'''(G) = -2\kappa p, \tag{5}$$

where $H = \frac{\dot{a}(t)}{a(t)}$ is the Hubble parameter and $\dot{a}(t) \equiv \frac{da}{dt}$.

Also, we have

$$R = 6(2H^2 + \dot{H}), \tag{6}$$

$$G = 24H^2(H^2 + \dot{H}). \tag{7}$$

In the present model, we are taking $F(R, G) = R + \alpha e^{-G}$ and this term denotes the difference with general relativity. Here α is an arbitrary positive constant.

B. Power law cosmology

To implement the power-law based cosmological model, we take the scale factor [62] as

$$a(t) = a_0(\frac{t}{t_0})^{\zeta}, \tag{8}$$

where a_0 represents the current value of the scale factor and ζ is a dimensionless parameter.

Now, the scale factor may be used to characterise the Hubble parameter as

$$H \equiv \frac{\dot{a}}{a} = \frac{\zeta}{t}, \tag{9}$$

$$H_0 = \frac{\zeta}{t_0}. \tag{10}$$

Additionally, the scale factor can be provided via the redshift as $a(t) = \frac{a_0}{1+z}$, where H takes the following form in terms of z:

$$H = H_0(1 + z)^{\frac{1}{\zeta}}. \tag{11}$$

We take into account cosmological characteristics like pressure, energy density, EOS parameter, Hubble parameter, deceleration parameter, etc. to comprehend the history of the universe. A dimensionless variable known as the deceleration parameter may be used to calculate the universe's acceleration or deceleration phase. The definition of the deceleration parameter q is

$$q = -\frac{\ddot{a}}{aH^2}. \tag{12}$$

Now, the following three cases may arise: (i) if $q > 0$, then the phase of the universe is decelerating, (ii) if $q < 0$, it is accelerating and (iii) if $q = 0$, it is expanding continuously. As a result, Eqs. (8) – (12) provide

$$q = \frac{1}{\zeta} - 1. \tag{13}$$

So, using the deceleration parameter q and redshift, we can describe the Hubble parameter as follows

$$H(z) = H_0(1 + z)^{(1+q)}. \tag{14}$$

Let us now get the expressions for the energy density and the pressure by solving Eqs. (4) and (5), which are given as

$$\rho = \frac{\alpha e^{24H_0^4 q(z+1)^{4q+4}}(24H_0^4 q(z+1)^{4q+4}(96H_0^4(q+1)(z+1)^{4q+4} - 1) + 1)}{2\kappa} + \frac{6H_0^2(z+1)^{2q+2}}{2\kappa}, \tag{15}$$

$$p = \frac{\alpha e^{24H_0^4 q(z+1)^{4q+4}}(24H_0^4 q(z+1)^{4q+4}(3072H_0^8 q(q+1)^2(z+1)^{8q+8} + 16H_0^4(q+1)(9q+5)(z+1)^{4q+4} + 1) - 1}{2\kappa} + \frac{2H_0^2(2q-1)(z+1)^{2q+2}}{2\kappa},$$

$$\omega = \frac{p}{\rho} \tag{16}$$

We accept α and κ as unity for further analysis, and we limit H_0 and q using three current observational data sets: $H(z)$, BAO and Pantheon compilation of SN Ia data.

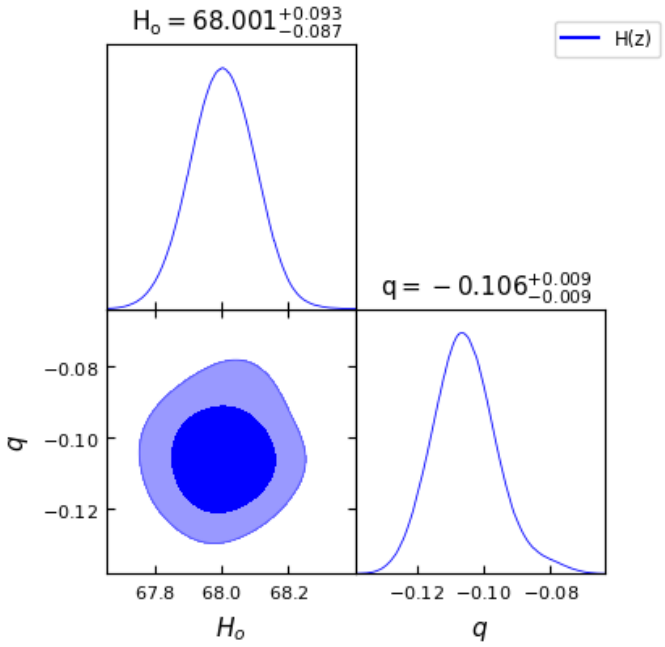

FIG. 1. In this figure we have exhibited one-dimensional marginalized distribution and two-dimensional contours by using the $H(z)$ dataset.

III. OBSERVATIONAL CONSTRAINTS ON MODEL PARAMETERS

In this section, observational data sets are utilised to restrict the values of H_0 and q that occur in the tilted Hubble parametrization. In this model, we employ the $H(z)$, BAO, and Pantheon data sets, as well as their combined data collections. The $H(z)$ data points are given in [63]. The information on BAO and Pantheon compilation of SN Ia data are sourced from [64] and [65–68] respectively.

A. Observed Hubble Data (OHD) set

We utilise the 57-point OHD data from [63]. The best-fit values of H_0 and q are now found using the standard chi-square test. The Chi-square is calculated as follows

$$\chi^2_{HD}(H_0, q) = \sum_{i=1}^{57} \frac{[H(H_0, q, z_i) - H_{obs}(z_i)]^2}{\sigma^2_{z_i}}, \tag{17}$$

where H_{obs} and $H(H_0, q, z_i)$ are respectively the observed and theoretical values and σ_{z_i} is the standard deviation at $H(z_i)$.

B. BAO Data set

Let us utilize BAO data to evaluate and verify the probable predictions of our cosmological models at various redshift values. This will obviously offer a unique method to examine the expansion parameters of the presently accelerating universe at low redshift values. Here the BAO dataset has been obtained from the current surveys, e.g. 6dFGS, SDSS and WiggleZ, spanning in the specific redshift range $0.106 < z < 0.73$. The basic idea behind this is as follows: the dimensionless amount serves to obtain a clear-cut indication of the primordial baryon-photon acoustic

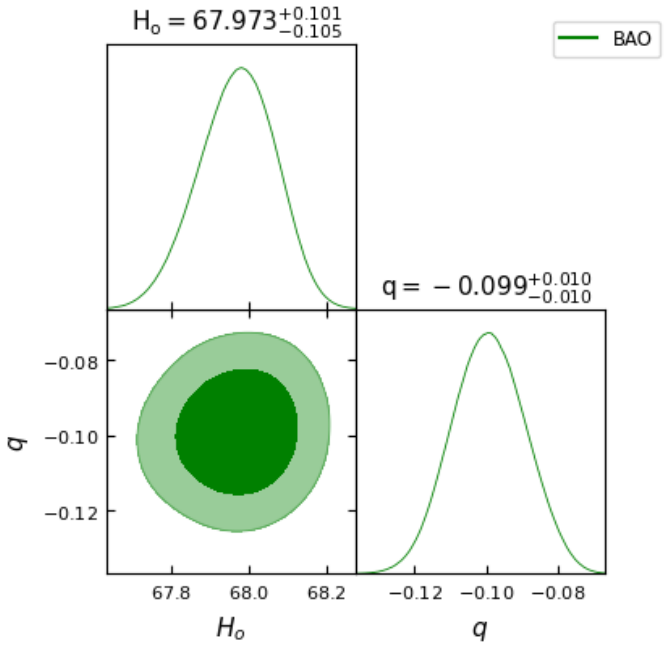

FIG. 2. In this figure we have exhibited one-dimensional marginalized distribution and two-dimensional contours by using the BAO dataset.

oscillations in the matter power spectrum. Hence

$$A(z) = \sqrt{\Omega_m}[H(z_i)/H_0]^{-1/3}\left[\frac{1}{z_i}\int_0^{z_i}\frac{H_0}{H(z)}dz\right]^{2/3}. \tag{18}$$

C. Pantheon Data set

For the redshift range of $0.01 < z < 2.26$, we utilise the Pantheon data compilation, which has 1048 data points. This data is taken from different supernovae survey, e.g. In the range of $0.01 < z < 0.07$, $0.01 < z < 0.06$, $0.03 < z < 0.40$, $0.12 < z < 1.06$, $0.02 < z < 0.63$, and $0.73 < z < 2.26$ respectively, CfA1 - 4, CSP, SDSS, SNLS, PS1, high z gives 147, 25, 335, 236, 279, 26 SN Ia for each Sample. The investigation of the expansion rate heavily relies on SNeIa. To assess the theoretically expected apparent magnitude (m) and absolute magnitude (M) with respect to colour and stretch, we thus compute the distance modulus $mu_T h(z_i)$ as follows

$$\mu(z) = -M + m = \mu_0 + 5logD_L(z), \tag{19}$$

where $D_L(z)$ and μ_0 are respectively the luminosity distance and the nuisance parameter.

These are given by

$$D_L(z) = cD_n(1+z)\int_0^z \frac{1}{H(z^*)}dz^*, \tag{20}$$

$$D_n(z) = \begin{cases} \frac{sinh(\sqrt{\Omega_m})}{H_0\sqrt{\Omega_m}}, \text{ for } \Omega_m > 0 \\ 1, \text{for } \Omega_m = 0 \\ \frac{sin(\sqrt{\Omega_m})}{H_0\sqrt{\Omega_m}}, \text{for } \Omega_m < 0 \end{cases} \tag{21}$$

$$\mu_0 = 5log\left(\frac{H_0^{-1}}{1Mpc}\right) + 25, \tag{22}$$

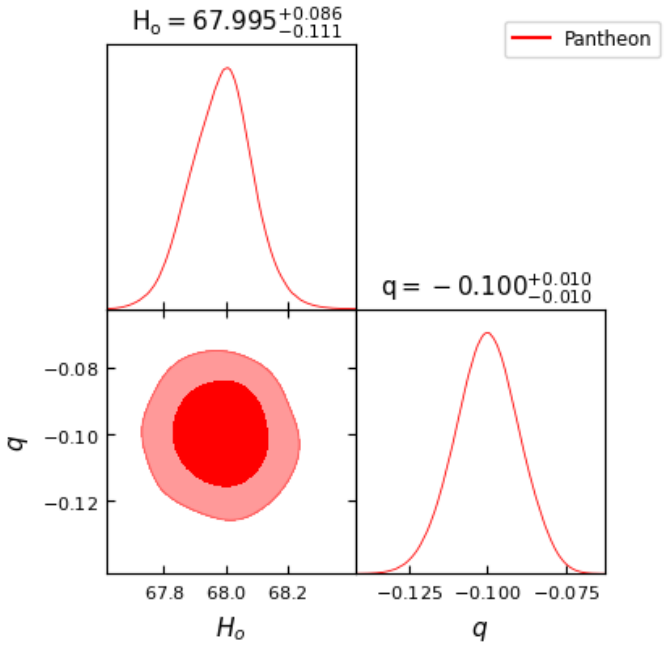

FIG. 3. In this figure we have exhibited one-dimensional marginalized distribution and two-dimensional contours by using the Pantheon dataset.

respectively.

Now, the minimum χ^2 function is given as

$$\chi^2_{Pan}(H_0, q) = \sum_{i=1}^{1048} \left[\frac{\mu_{th}(H_0, q, z_i) - \mu_{obs}(z_i)}{\sigma_\mu(z_i)} \right]^2. \tag{23}$$

D. Joint OHD + Pantheon Data set

By performing joint statistical analysis using $H(z)$ and Pantheon data sets, we obtain stronger constraints. Therefore, the chi-sq function for joint data sets can be written as

$$\chi^2_{Joint} = \chi^2_{OHD} + \chi^2_{PAN}. \tag{24}$$

E. Joint OHD + BAO + Pantheon Data set

By performing joint statistical analysis using $H(z)$, BAO and Pantheon data sets, we obtain even stronger and more reliable constraints. Therefore, the chi-sq function for joint data sets can be written as

$$\chi^2_{Joint} = \chi^2_{OHD} + \chi^2_{BAO} + \chi^2_{PAN}. \tag{25}$$

IV. RESULTS UNDER THE $f(R, G)$ GRAVITY MODEL

A. Parameter Estimation

The two-dimensional contour plots for H_0 and q parameter using the data sets OHD, BAO, Pantheon and their combinations OHD + Pantheon and OHD + BAO + Pantheon are shown in the Figs. 1, 2, 3, 4 and 5 respectively.

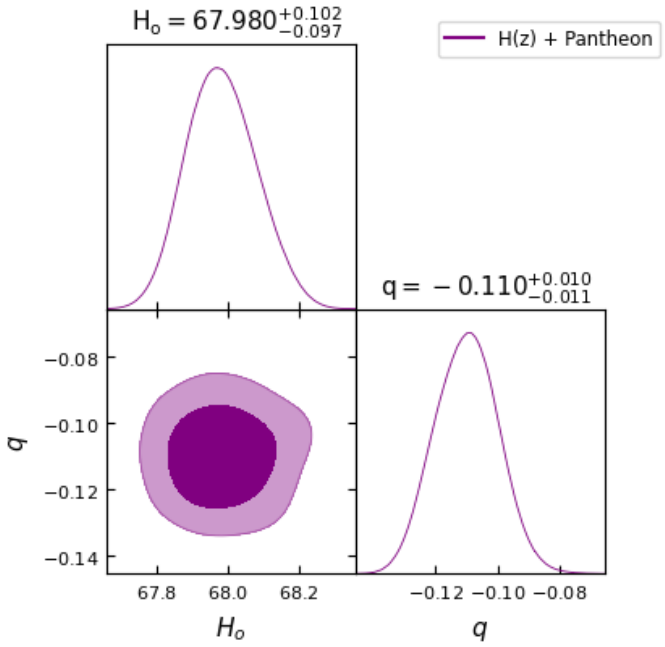

FIG. 4. In this figure we have exhibited one-dimensional marginalized distribution and two-dimensional contours by using the combination of $H(z)$ and Pantheon dataset.

TABLE I. The parameter values exstructed from different datasets (i.e. H(z), BAO, Pantheon, H(z) + Pantheon, H(z) + BAO + Pantheon). We have executed here MCMC and Bayesian analysis.

Parameter	H(z)	BAO	Pantheon	H(z) + Pantheon	H(z) + BAO + Pantheon
H_0	$68.001^{+0.093}_{-0.087}$	$67.973^{+0.101}_{-0.105}$	$67.995^{+0.0866}_{-0.111}$	$67.980^{+0.102}_{-0.097}$	$68.018^{+0.093}_{-0.104}$
q	$-0.106^{+0.009}_{-0.009}$	$-0.099^{+0.010}_{-0.010}$	$-0.100^{+0.010}_{-0.010}$	$-0.110^{+0.010}_{-0.011}$	$-0.104^{+0.010}_{-0.011}$

Their combined nature can be seen in Fig. 6. The obtained values of H_0 and q parameters by implementing the data sets are presented in Table I. We observe that the obtained values of parameter q are negative, indicating $q < 0$, which clearly gives the indication of an accelerating universe, as discussed in the theory section.

B. Energy Conditions

Energy conditions (ECs) or similarly construct cosmic principles that explain the distribution of matter and energy across the universe. They are based on Einstein's gravitational equations and replicate the rules of the cosmos. These circumstances indicate the distribution of matter and energy in space. Hence the energy conditions can be expressed as follows:

i) Weak Energy Condition (WEC): $\rho \geq 0$,

ii) Null Energy Condition (NEC): $\rho - p \geq 0$,

iii) Strong Energy Condition (SEC): $\rho + 3p \geq 0$,

iv) Dominant Energy Condition (DEC): $\rho + p \geq 0$.

All the energy conditions seperately as well as jointly are shown in Figs. 15, 16, 17, 18 and 19 using the Bayesian Analysis of the parameters. Except for Strong Energy Condition (SEC), our results show that Null Energy Condition

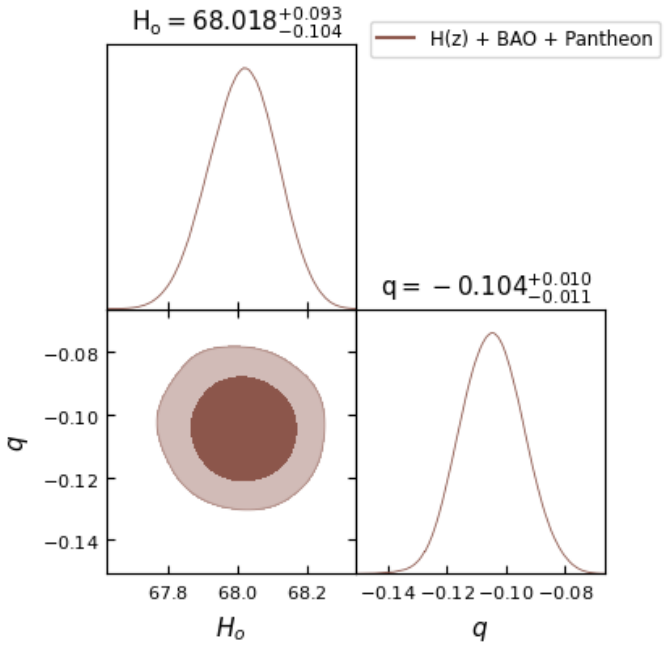

FIG. 5. In this figure we have exhibited one-dimensional marginalized distribution and two-dimensional contours by using the combination of $H(z)$, BAO and Pantheon dataset.

(NEC), Weak Energy Condition (WEC), and Dominant Energy Condition (DEC) are all satisfied. The SEC violation is justified by the universe's fast growth. Therefore, the $f(R, G)$ theory of gravity has potential to explain the current scenario of the late-time acceleration without any need for the cosmological constant as well dark energy in the universe's energy content. It is to note that the distribution of the energy density ρ with respect to time t is shown in Fig. 7, whereas the distribution of the pressure is shown in Fig. 8.

C. State Finder Diagnotics

Basically, state finder diagnostics help us to obtain hidden features of the status of dark energy and thus mysteries attached to the history of the universe. As we employ a cosmic compass, these diagnostics lead us through the complexities of cosmic evolution. The r and s parameters are used in state finder diagnostics. Using these characteristics, we can gain a better understanding of the evolution of the universe. Consider them cosmic metres that offer data on the expansion of the universe and its constituent components. These are basically dimensionless parameters which encapsulate the essence of the cosmic development and thus serve as a filter to aid in our understanding of the underlying dynamics of the universe.

Now, the general mathematical expression for the required parameter, expressed in terms of H, is as follows:

$$r = \frac{\dddot{a}}{aH^3}, \tag{26}$$

whereas the equations for r and s in our model, when expressed in terms of q, become

$$r = 2q^2 + q, \tag{27}$$

$$s = \frac{-1 + r}{3(-\frac{1}{2} + q)}. \tag{28}$$

The scale factor trajectories in the resulting model may be shown in Fig. 10 to follow a specific set of paths. Our strategy is consistent with the results for the cosmic diagnostic pair from power law cosmology.

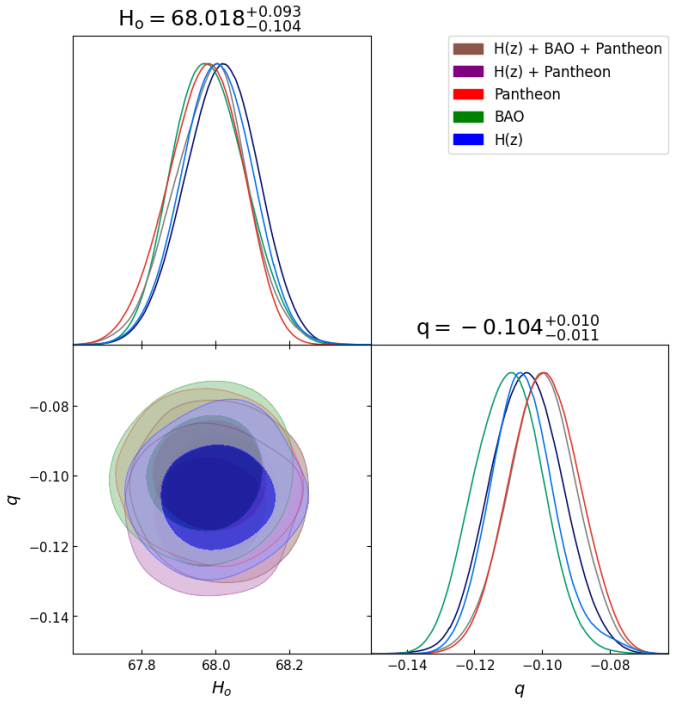

FIG. 6. In this figure we have exhibited one-dimensional marginalized distribution and two-dimensional contours by using the combined variability across all dataset combinations.

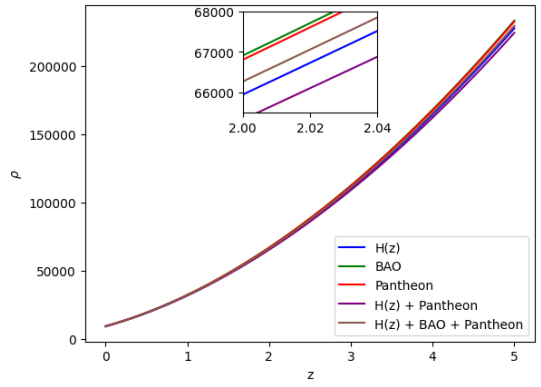

FIG. 7. In this figure we have exhibited the dynamic variation of the energy density (ρ) over the redshift (z) under various parameter conditions derived from distinct combinations of the $H(z)$, BAO and Pantheon datasets.

D. Om(z) parameter

When assessing various dark energy hypotheses in academic works, researchers commonly use the state finder parameters $r - s$ and the Om diagnosis. The important $Om(z)$ parameter is formed when the Hubble parameter H and the cosmic redshift z combine which can be defined as

$$Om(z) = \frac{[\frac{H(z)}{H_0}]^2 - 1}{(1+z)^3 - 1}, \tag{29}$$

where H_0 corresponds to the current value of the Hubble parameter. According to Shahalam et al. [69], the negative, zero, and positive values of $Om(z)$ indicate the quintessence ($\omega \geq -1$), ΛCDM, and phantom ($\omega \leq -1$) dark energy (DE) hypotheses, respectively.

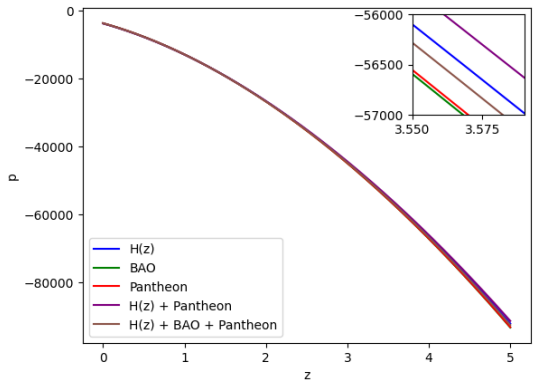

FIG. 8. In this figure we have exhibited the dynamic variation of the pressure (p) over the redshift (z) under various parameter conditions derived from distinct combinations of the $H(z)$, BAO and Pantheon datasets.

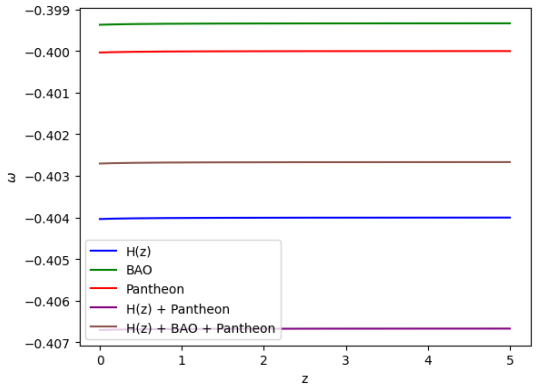

FIG. 9. In this figure we have exhibited variation of the equation of state parameter (ω) vs the redshift (z) which demonstrates that dark energy contributes to the accelerated expansion of the universe, however with a bit variations with the redshift and thus potentially leading to interesting cosmological consequences.

The $Om(z)$ parameter can be provided for our model as follows:

$$Om(z) = \frac{(1+z)^{2/b} - 1}{(1+z)^3 - 1}. \tag{30}$$

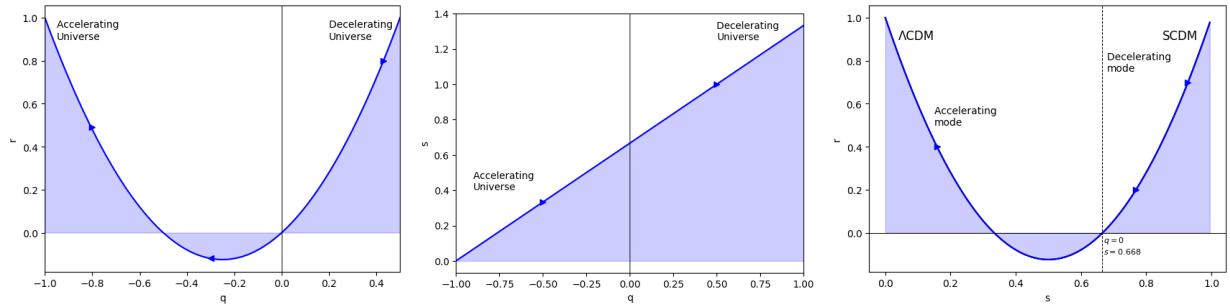

FIG. 10. In this figure we have exhibited the features of the State Finder plots of $r-q$, $s-q$ and $r-q$.

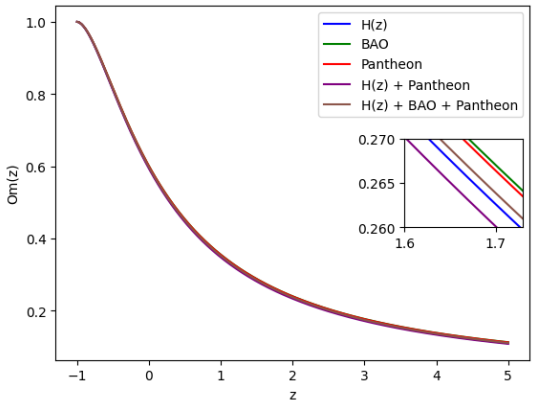

FIG. 11. In this figure we have exhibited variations of $Om(z)$ with z across for different combined datasets by considering the β values obtained from each dataset.

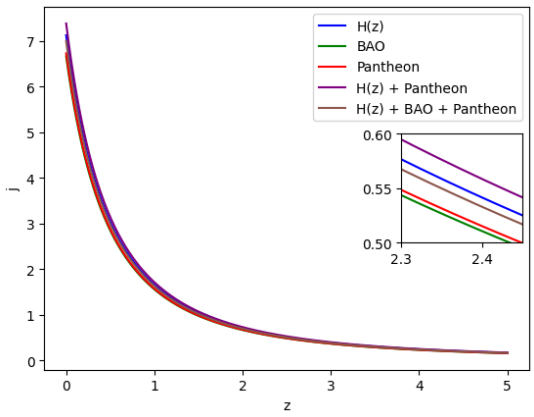

FIG. 12. In this figure we have exhibited the feature of the Jerk parameter j vs z. Here values of j at $z = 0$ are as follows: for $H(z)$ = 7.127 s^{-3}, for BAO = 6.663 s^{-3}, for Pantheon = 6.731 s^{-3}, for $H(z)$ + Pantheon = 7.387 s^{-3} and for $H(z)$ + BAO + Pantheon = 6.997 s^{-3}

E. Cosmographic Parameters

Many cosmological parameters, given as higher-order derivatives of the scalar component, are examined to comprehend the universe's expansion history better. As a result, these characteristics are extremely useful for investigating the dynamics of the cosmos. For example, the Hubble parameter H depicts the universe's expansion rate, the deceleration parameter q depicts the universe's phase transition whereas the jerk parameter j, snap parameter s and lerk parameter l are required to study dark energy theories and their dynamics. These are as follows:

$$H = \frac{\dot{a}}{a} \tag{31}$$

$$q = \frac{\ddot{a}}{aH^2} \tag{32}$$

$$j = \frac{\dddot{a}}{aH^3} \tag{33}$$

$$s = \frac{\ddddot{a}}{aH^4} \tag{34}$$

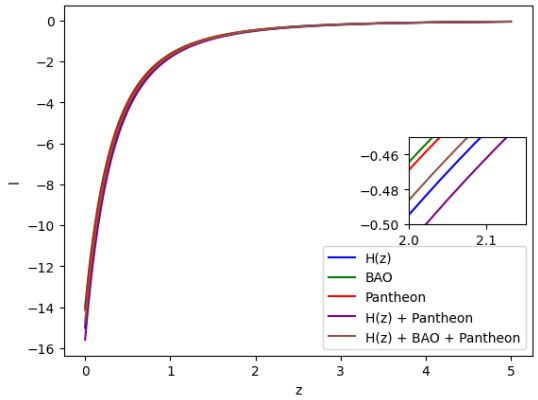

FIG. 13. In this figure we have exhibited the feature of the Lerk parameter l vs z.

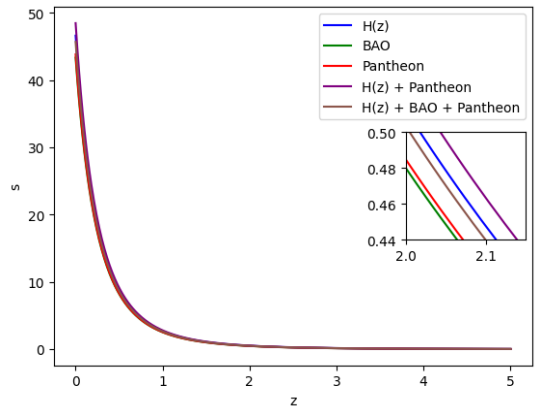

FIG. 14. In this figure we have exhibited the feature of the Snap parameter s vs z.

$$l = \frac{\dddot{a}}{aH^5} \tag{35}$$

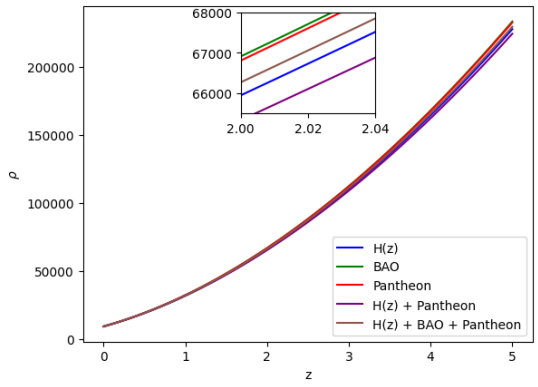

FIG. 15. In this figure we have exhibited the Weak Energy Conditions (WEC) vs the redshift (z) for all the combined datasets.

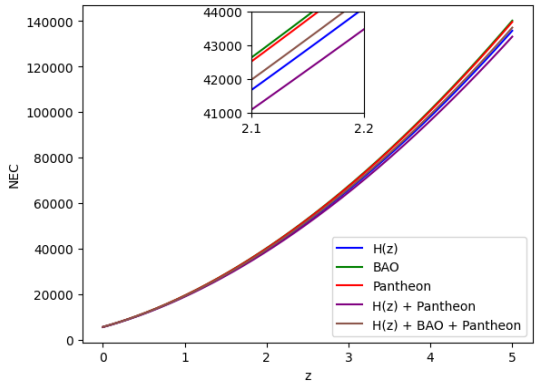

FIG. 16. In this figure we have exhibited the Null Energy Conditions (NEC) vs the redshift (z) for all the combined datasets.

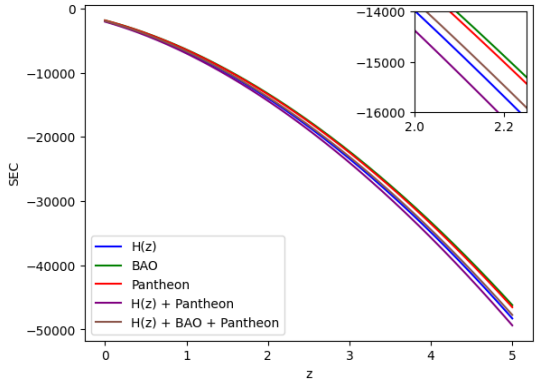

FIG. 17. In this figure we have exhibited the Strong Energy Conditions (SEC) vs the redshift (z) for all the combined datasets.

V. DISCUSSION AND CONCLUSION

The motivation behind the research paper was to examine the Ricci scalar R and the Gauss-Bonnet invariant G to characterize a cosmological model in flat space-time via $f(R, G)$ gravity. Here we wanted to investigate the observational limitations under a power law cosmology that relies on two parameters - H_0 (the Hubble constant) and q (the deceleration parameter) utilizing the 57-point $H(z)$ data, 8-point BAO data, 1048-point Pantheon data, joint data of $H(z)$ + Pantheon and joint data of $H(z)$ + BAO + Pantheon. The outcomes for H_0 and q are realistic

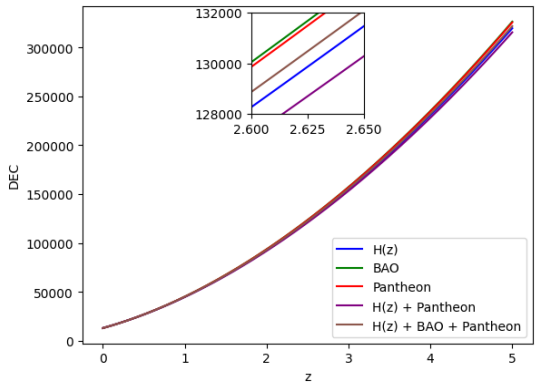

FIG. 18. In this figure we have exhibited the Dominant Energy Conditions (DEC) vs the redshift (z) for all the combined datasets.

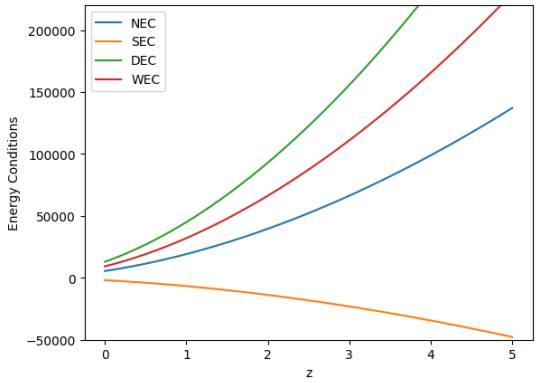

FIG. 19. In this figure we have exhibited all the energy conditions vs time.

within observational ranges. As can be noted that our estimate of H_0 is remarkably consistent with various recent Planck Collaboration studies under the ΛCDM model.

We have shown via several graphical demonstrations (Figs. 1 - 19 and Table I) that the obtained values for H_o and q satisfactorily correspond to the results observed by the Plank collaboration group. Along with this graphical presentation we have also analyzed the model by studying the energy conditions, the jerk parameter, the lerk parameter and the Om diagnostics as well as the state finder diagnostic tools. According to our study, the power law cosmology within the context of $f(R,G)$ gravity provides the most comprehensive explanation for the important aspects of cosmic evolution. Furthermore, at the final stage of this paper, we have seen the work of Singh et al. [70] that prescribes for a cosmological model with power law under the framework of modified theory with higher order curvature term. They [70] have obtained $H_0 = 68.119^{+0.028}_{-0.12}$ $km\ s^{-1}Mpc^{-1}$, $q = -0.109^{+0.014}_{-0.014}$; $H_0 = 70.5^{+1.3}_{-0.98}$ $km\ s^{-1}Mpc^{-1}$, $q = -0.25^{+0.15}_{-0.15}$ and $H_0 = 69.103^{+0.019}_{-0.10}$ $km\ s^{-1}Mpc^{-1}$, $q = -0.132^{+0.014}_{-0.014}$ by using $H(z)$ data, Pantheon compilation of SN Ia data and joint data of H(z) + Pantheon respectively. In this paper, the constrained values from the proposed model are as follows: $H_0 = 68.001^{+0.093}_{-0.087}$ km s^{-1} Mpc^{-1}, $q = -0.106^{+0.009}_{-0.009}$; $H_0 = 67.973^{+0.101}_{-0.105}$ km s^{-1} Mpc^{-1}, $q = -0.099^{+0.010}_{-0.010}$; $H_0 = 67.995^{+0.086}_{-0.111}$ km s^{-1} Mpc^{-1}, $q = -0.100^{+0.010}_{-0.010}$; $H_0 = 67.980^{+0.012}_{-0.097}$ km s^{-1} Mpc^{-1}, $q = -0.110^{+0.010}_{-0.011}$; $H_0 = 68.018^{+0.093}_{-0.104}$ km s^{-1} Mpc^{-1}, $q = -0.104^{+0.010}_{-0.011}$ by using $H(z)$ data, 8-point BAO data, 1048-point Pantheon data, joint data of $H(z)$ + Pantheon and joint data of $H(z)$ + BAO + Pantheon respectively. As a suitable methodology the welknown and effective Markov Chain Monte Carlo (MCMC) has been uniquely employed in the present investigatin.

At this point it is worthwhile to mention that the proposed model has been minimized H_0 tensions and it is calibrated only 0.68σ, 1.19σ, 1.191σ, 1.23σ and 1.17σ for $H(z)$ data, 8-point BAO data, 1048-point Pantheon data, joint data of $H(z)$ + Pantheon and joint data of $H(z)$ + BAO + Pantheon respectively when we analyzed the estimated values of H_0 in this paper with the value of H_0 obtained by Plank Collaboration [48]. Moreover, because of the constant value of deceleration parameter q in power-law cosmology, it could not able to describe the red-shift transition and the proposed model fails to explain the early deceleration phase of the universe. However, one can describes the early deceleration phase of the universe by choosing appropriate value of ζ in $q = \frac{1}{\zeta} - 1$. But at the same time one can note that the model fails to explain the late-time acceleration of the universe. Finally, even though we obtaine so many useful features, the power-law cosmology seems not a completely packagable technique to study to entire dynamics and eventual fate of the universe.

DATA AVAILABILITY

In the present study, we have used available observational data only where no data has been produced in any new form.

CONFLICT OF INTEREST

The authors declare no conflict of interest.

ACKNOWLEDGEMENT

SR gratefully acknowledges support from the Inter-University Centre for Astronomy and Astrophysics (IUCAA), Pune, India under its Visiting Research Associateship Programme as well as the facilities under ICARD, Pune at CCASS, GLA University, Mathura, India. LKS is also thankful to IUCAA for approving a short visit there when the idea of the present work has been conceived.

[1] S. Nojiri, S. D. Odintsov and P. V. Tretyakov, Prog. Theor. Phys. Suppl. **172**, 81 (2008).
[2] G. Cognola, M. Gastaldi and S. Zerbini, Int. J. Theor. Phys. **47**, 898 (2008).
[3] K. Bamba, Cosmological Issues in $F(T)$ Gravity Theory, arXiv:1504.04457 [gr-qc].
[4] S. D. Odintsov, V. K. Oikonomou and S. Banerjee, Nucl. Phys. B **938**, 935 (2019).
[5] A. K. Yadav, F. Rahaman and S. Ray, Int. J. Theor. Phys. **50**, 871 (2011).
[6] A. K. Yadav, Astrophys. Space Sci. **335**, 565 (2011).
[7] F. G. Alvarenga, A. de la Cruz-Dombriz, M. J. S. Houndjo, M. E. Rodrigues and D. Sáez-Gómez, Phys. Rev. D **87**, 103526 (2013).
[8] A. Das, F. Rahaman, B. K. Guha and S. Ray, Eur. Phys. J. C **76**, 654 (2016).
[9] M. E. S. Alves, P. H. R. S. Moraes, J. C. N. de Araujo and M. Malheiro, Phys. Rev. D **94**, 024032 (2016).
[10] A. K. Yadav, Astrophys. Space Sci. **361**, 276 (2016).
[11] Z. Yousaf, K. Bamba and M. Z. U. H. Bhatti, Phys. Rev. D **93**, 124048 (2016).
[12] A. Das, S. Ghosh, B. K. Guha, S. Das, F. Rahaman and S. Ray, Phys. Rev. D **95**, 124011 (2017).
[13] D. Deb, F. Rahaman, S. Ray, B. K. Guha, Phys. Rev. D **97**, 084026 (2018).
[14] D. Deb, S. V. Ketov, S. K. Maurya, M. Khlopov, P. H. R. S. Moraes and S. Ray, Mon. Not. R. Astron. Soc. **485**, 5652 (2018).
[15] L. K. Sharma, A. K. Yadav, P. K. Sahoo and B. K. Singh, Res. Phys. **10**, 738 (2018).
[16] R. Nagpal, S. K. J. Pacif, J. K. Singh, K. Bamba and A. Beesham, Eur. Phys. J. C **78**, 946 (2018).
[17] L. K. Sharma, A. K. Yadav and B. K. Singh, New Astron. **79**, 101396 (2020).
[18] L. K. Sharma, B. K. Singh and A. K. Yadav, Int. J. Geom. Meth. Mod. Phys. **17**, 2050111 (2020).
[19] D. Deb, S. V. Ketov, M. Khlopov and S. Ray, J. Cosmol. Astropart. Phys. **10**, 070 (2019).
[20] D. Deb, F. Rahaman, S. Ray and B. K. Guha, J. Cosmol. Astropart. Phys. **03**, 044 (2019).
[21] S. Biswas, S. Ghosh, B. K. Guha, F. Rahaman and S. Ray, Ann. Phys. **401**, 1 (2019).
[22] S. Biswas, D. Shee, S. Ray and B. K. Guha, Eur. Phys. J C **80**, 175 (2020).
[23] A. K. Yadav, L. K. Sharma, B. K. Singh and P. K. Sahoo, New Astron. **78**, 101382 (2020).
[24] S. Biswas, D. Deb, S. Ray and B. K. Guha, Ann. Phys. **428**, 168429 (2021).
[25] S. K. Tripathy, B. Mishra, M. Khlopov and S. Ray, Int. J. Mod. Phys. D **30**, 2140005 (2021).
[26] S. K. Maurya, F. Tello-Ortiz and S. Ray, Phys. Dark Univ. **31**, 100753 (2021).
[27] A. Singh, Eur. Phys. J. C **83**, 696 (2023).
[28] K. Bamba, S. Capozziello, S. Nojiri, S. D. Odintsov, 2012, Astrophys. Space Sci. **342**, 155 (2012).
[29] S. Nojiri, S. D. Odintsov and O. G. Gorbunova, J. Phys. A **39**, 6627 (2006).
[30] S. Nojiri and S. D. Odintsov, Phys. Lett. B **631**, 1 (2005).
[31] G. Cognola, E. Elizalde, S. Nojiri, S. D. Odintsov and S. Zerbini, Phys. Rev. D **73**, 084007 (2006).
[32] B. Li, J. D. Barrow and D. F. Mota, Phys. Rev. D **76**, 044027 (2007).
[33] E. Elizalde, R. Myrzakulov, V. V. Obukhov and D. Saez-Gomez, Class. Quant. Grav. **27**, 095007 (2010).
[34] N. M. Garcia, F. S. N. Lobo, J. P. Mimoso and T. Harko, J. Phys. Conf. Ser. **314**, 012056 (2011).
[35] K. Izumi, Phys. Rev. D **90**, 044037 (2014).
[36] K. Bamba, A. N. Makarenko, A. N. Myagky and S. D. Odintsov, Phys. Lett. B **732**, 349 (2014).
[37] A. Escofet and E. Elizalde, Mod. Phys. Lett. A **31**, 1650108 (2016).
[38] V. K. Oikonomou, Phys. Rev. D **92**, 124027 (2015).
[39] V. K. Oikonomou, Astrophys. Space Sci. **361**, 211 (2016).
[40] A. N. Makarenko, Int. J. Geom. Meth. Mod. Phys. **13**, 1630006 (2016).

[41] A. N. Makarenko and A. N. Myagky, Int. J. Geom. Meth. Mod. Phys. **14**, 1750148 (2017).
[42] K. Kleidis and V. K. Oikonomou, Int. J. Geom. Meth. Mod. Phys. **15**, 1850064 (2017).
[43] D. Lohiya and M. Sethi, Class. Quant. Grav. **16**, 1545 (1999).
[44] M. Sethi, A. Batra and D. Lohiya, Phys. Rev. D **60**, 108301 (1999).
[45] A. Batra, D. Lohiya, S. Mahajan and A. Mukherjee, Int. J. Mod. Phys. D **9**, 757 (2000).
[46] Z. H. Zhu, M. Hu, J. S. Alcaniz and Y. X. Liu, Astron. Astrophys. **483**, 15 (2008).
[47] A. G. Riess et al., Astrophys. J. Lett. **934**, L7 (2022).
[48] N. Aghanim et al. [Planck Collaboration], Astron. Astrophys. **641**, A6, 2020.
[49] E. Abdalla et al., JHEAp **34,** 49 (2022).
[50] L. Perivolaropoulos and F. Skara, New Astron. Rev. **95**, 101659 (2022).
[51] S. Kumar and R. C. Nunes, Phys. Rev. D **94**, 123511 (2016).
[52] S. Kumar, R. C. Nunes, and S. K. Yadav, Eur. Phys. J. C **79**, 576 (2019).
[53] S. Kumar, Phys. Dark Univ. **33**, 100862 (2021).
[54] J. C. N. de Araujo, A. De Felice, S. Kumar, and R. C. Nunes, Phys. Rev. D **104**, 104057 (2021).
[55] J. P. Hu and F.-Y. Wang, Hubble Tension: Universe **9**, 94 (2023).
[56] S. Vagnozzi, Universe **9**, 393 (2023).
[57] P. Kroupa, E. Gjergo, E. Asencio, M. Haslbauer, J. Pflamm-Altenburg, N. Wittenburg, N. Samaras, I. Thies, and W. Oehm, arXiv:2309.11552.
[58] A. Bernui, E. Di Valentino, W. Giar'e, S. Kumar, and R. C. Nunes, Phys. Rev. D **107**, 103531 (2023).
[59] O. Akarsu, S. Kumar, E. Â¨OzÂ¨ulker, and J. A. Vazquez, Phys. Rev. D **104**, 123512 (2021).
[60] O. Akarsu, S. Kumar, E. Â¨OzÂ¨ulker, J. A. Vazquez, and A. Yadav, Phys. Rev. D **108**, 023513 (2023).
[61] O. Akarsu, E. Di Valentino, S. Kumar, R. C. Nunes, J. A. Vazquez, and A. Yadav, arXiv:2307.10899.
[62] S. Kumar, Mon. Not. R. Astron. Soc. **422**, 2532 (2012).
[63] A. Bouali, H. Chaudhary, T. Harko, F. S. N. Lobo, T. Ouali and M. A. S. Pinto, Mon. Not. R. Astron. Soc. **526**, 4192 (2023).
[64] S. Alam, et al., Phys. Rev. D **103**, 083533 (2021).
[65] D. M. Scolnic et al. [Pan-STARRS1], Astrophys. J. **859**, 101 (2018).
[66] S. Jha, R. P. Kirshner, P. Challis, P. M. Garnavich, T. Matheson, A. M. Soderberg, G. J. M. Graves, M. Hicken, J. F. Alves and H. G. Arce, et al. Astron. J. **131**, 527 (2006).
[67] M. Hicken, P. Challis, S. Jha, R. P. Kirsher, T. Matheson, M. Modjaz, A. Rest and W. M. Wood-Vasey, Astrophys. J. **700**, 331 (2009).
[68] C. Contreras, M. Hamuy, M. M. Phillips, G. Folatelli, N. B. Suntze, S. E. Persson, M. Stritzinger, L. Boldt, S. Gonzalez and W. Krzeminski, et al. Astron. J. **139**, 519 (2010).
[69] M. Shahalam, S. Sami and A. Agarwa, Mon. Not. R. Astron. Soc. **448**, 2948 (2015).
[70] J. K. Singh, Shaily, A. Pradhan, A. Beesham, arXiv: 2304.09917.